Proceedings of the IEEE Conf. on Decision and Control, Orlando, FL, 2011

Limit Cycles in Replicator-Mutator Network Dynamics

Darren Pais and Naomi Ehrich Leonard

***Abstract*— The replicator-mutator equations from evolutionary dynamics serve as a model for the evolution of language, behavioral dynamics in social networks, and decision-making dynamics in networked multi-agent systems. Analysis of the stable equilibria of these dynamics has been a focus in the literature, where symmetry in fitness functions is typically assumed. We explore asymmetry in fitness and show that the replicator-mutator equations exhibit Hopf bifurcations and limit cycles. We prove conditions for the existence of stable limit cycles for the dynamics in the case of circulant fitness matrices, and illustrate their existence in the noncirculant case. For decision-making networks, these limit cycles correspond to sustained oscillations in decisions across the group.**

I. INTRODUCTION

In this paper we study the replicator-mutator equations from evolutionary dynamics; these serve as a model for the evolution of language [1], for behavior selection in social networks [2], [3], and also for decision-making dynamics in networked multi-agent systems [4]. Our main result is to prove a Hopf bifurcation for these dynamics with certain network interconnection topologies; this implies the existence of limit cycle behavior. For decision-making networks, the limit cycles correspond to sustained oscillations in decisions across the group.

Evolutionary dynamics [5], [6], [7] are, broadly speaking, an effort to cast the basic tenets of Darwinian natural selection (replication, competition, strategy dependent fitness, mutation) in a mathematical framework. The set of replicator equations [8] are the simplest model of evolutionary dynamics for a population divided among a finite set of N competing strategies ($N \geq 2$). The differential equations model the game theoretic interactions among the sub-populations, each subscribed to a different competing strategy, and determine how the different sub-populations change in size as a consequence of these interactions.

Although the replicator dynamics have proved to be a powerful tool in analyzing a variety of classical games from an evolutionary perspective, they do not model mutation, a key ingredient of selection theory. Mutation can be included by adding the possibility that individuals spontaneously change from one strategy to another. This yields the replicator-mutator dynamics [9], which have played a prominent role in evolutionary theory and have recently been employed to model social and multi-agent network dynamics [2]. The replicator-mutator dynamics can be interpreted from a graph theoretic perspective by representing the strategies as nodes of the graph, and representing payoffs for interactions between strategies as graph edge weights [10].

We are motivated in particular by three applications of the replicator-mutator equations which we now briefly describe.

a) The replicator-mutator dynamics have been used in the development of a mathematical framework for the evolution of language [1]. A key result is the bifurcation of the equilibria from a state where several grammars coexist in a population to a state of high grammatical coherence as mutations in the population decrease [11], [12], [13].

b) In a recent paper [2], Olfati-Saber proposed an adaptation of the replicator-mutator model to look at the role of dominance in social networks. Simulations of the evolutionary social network model show a transition from the dominance of a single strategy, to the coexistence of a few strategies, to eventually the collapse of dominance, as the extent of mutation in the network increases.

c) We are also motivated by decision-making dynamics in networked multi-agent systems. In this context, it has been shown that simple models with pairwise interactions between agents and noisy imitation of successful strategies evaluate (under certain conditions) to the replicator-mutator dynamics [14], [15], [16]. Recent papers have employed the replicator-mutator equations to model wireless multi-agent networks [17], [4].

The analysis of the replicator-mutator dynamics in the literature has focused primarily on stable limiting equilibrium behavior for undirected payoff graphs. However, the $N = 2$ analysis in [18] shows that directed graphs yield qualitatively different bifurcations from undirected graphs. Further, in [19] the authors illustrate that the replicator-mutator dynamics exhibit limit cycles and chaos for specific model parameter values. Motivated by this, we focus our analysis on proving conditions under which the dynamics converge to stable limit cycles for $N = 3$ strategies. We show that the limiting behaviors of the replicator-mutator dynamics are tied to the structure of the payoff graph, and that breaking symmetry, from undirected to directed (particularly circulant) graphs, yields some of the richer outcomes simulated in [19].

As noted in [19], oscillations appear to be more realistic than stable equilibria for the language dynamics with timescales on the order of several centuries. Our work shows that such oscillations can exist in broad regions of payoff parameter space. For social networks, our results show that certain directed networks can yield rich behavioral outcomes such as preference oscillations. For decision making in multi-agent systems, our results address the exploration versus exploitation tradeoff: small mutations favor fast convergence

This work is supported in part by ONR grant N00014-09-1-1074 and AFOSR grant FA9550-07-1-0-0528. D. Pais is also supported by the Britt and Eli Harari graduate fellowship.

D. Pais and N. E. Leonard are with the Department of Mechanical and Aerospace Engineering, Princeton University, Princeton, NJ 08544, USA. {dpais,naomi}@princeton.edu

to a decision (exploitation) whereas large mutations favor exploration of the decision space. Intermediate mutation strength can lead to limit cycles, which enable efficient examination of alternative choices.

Section II provides the details of the replicator-mutator model. Bifurcation plots for the model with $N = 2$ and $N = 3$ strategies are computed in Section III. We prove the Hopf bifurcations for $N = 3$ and circulant payoffs in Section IV and consider non-circulant payoffs in Section V. In Section VI we conclude and discuss future directions.

II. MODEL

A. Replicator-Mutator Dynamics

For a large population of agents distributed among N possible strategies S_i, $i = 1, 2, \cdots, N$, the replicator-mutator dynamics are given by

$$\dot{x}_i = \sum_{j=1}^{N} x_j f_j(\boldsymbol{x}) q_{ji} - x_i \phi =: g_i(\boldsymbol{x}); \quad \phi = \boldsymbol{f}^T \boldsymbol{x}. \tag{1}$$

Here, x_i is the fraction of the population with strategy S_i and fitness f_i, ϕ is the average population fitness, and q_{ij} is the probability that agents mutate (spontaneously change) from strategy S_i to S_j. The fitness of agents with strategy S_i is given by

$$f_i = \sum_{k=1}^{N} b_{ik} x_k, \text{ or in matrix form, } \boldsymbol{f} = B\boldsymbol{x}. \tag{2}$$

$B = [b_{ij}] \in \mathbb{R}^{N \times N}$ is known as the payoff matrix where $b_{ij} \geq 0$ represents the payoff to an agent with strategy S_i on interacting with an agent with strategy S_j. We assume that payoffs are all nonnegative and that agents get a maximal payoff (normalized to 1) on interacting with others subscribed to the same strategy. Hence B satisfies

$$b_{ii} = 1 \text{ and } b_{ij} \in [0, 1) \text{ for } i \neq j. \tag{3}$$

As noted in [2], the payoff matrix B can be interpreted from a graph theoretic perspective as the adjacency matrix of a directed graph. The diagonal elements of B ($b_{ii} = 1$) correspond to self cycles at each node. Symmetric payoff matrices B correspond to undirected graphs.

Condition 1: Every row and column of B has at least one nonzero off diagonal element.

From the graph theoretic perspective, Condition 1 requires that every node of the graph has at least one outgoing and one incoming link; this ensures that there are no isolated disconnected nodes of the payoff graph. We will restrict to examining graphs that satisfy Condition 1.

Since $\sum_j q_{ij} = 1$, the mutation matrix $Q = [q_{ij}]$ is row stochastic. In this paper, we define the mutation probabilities q_{ij} as a function of the mutation strength μ as follows:

$$q_{ii} = (1 - \mu), \quad q_{ij} = \frac{\mu b_{ij}}{\sum_{i \neq j} b_{ij}} \text{ for } i \neq j. \tag{4}$$

The parameter $\mu \in [0, 1]$ represents the probability of error in replication. For example, $\mu = 0$ denotes perfect replication and no mutation whereas $\mu = 1$ denotes pure mutation. The choice of mutation propabilities q_{ij} in (4) is motivated by the graph theoretic perspective on the replicator-mutator dynamics and is a generalization of the structured mutational models in [10], [18]. Intuitively, this model implies that spontaneous mutation to alternative strategies is weighted in favor of strategies that yield higher payoff. Note that the mutation models in [2], [10], [12], [1] are special cases of (4) in which the payoff matrices B are symmetric.

The strategies S_i and payoffs b_{ij} can be interpreted in each of our motivating contexts:

a) For the evolution of language, each S_i is a specific grammar in the population and b_{ij} is the probability that a sentence spoken at random by individuals with grammar S_j can be parsed by individuals with grammar S_i.
b) In social networks, each S_i represents a particular behavior in a population and b_{ij} represents the degree to which agents with behavior S_i are attracted to behavior S_j.
c) In multi-agent decision making, each S_i represents an alternative choice for the group and the b_{ij} represent the perceived relative advantage of choice S_j for agents currently subscribed to choice S_i.

In [19] the authors consider specific instances of *asymmetric* payoff matrices and, using simulations, illustrate stable limit cycles and chaotic attractors for the replicator-mutator dynamics as a consequence. In this work we explore this effect and prove Hopf bifurcations for circulant asymmetric graphs in the case $N = 3$.

B. Dynamics on Simplices

Let $\boldsymbol{g}(\boldsymbol{x}) : \mathbb{R}^N \to \mathbb{R}^N$ be $\boldsymbol{g}(\boldsymbol{x}) = [g_1(\boldsymbol{x}), \cdots, g_N(\boldsymbol{x})]^T$. Define the n-simplex as

$$\Delta_n = \left\{ \boldsymbol{x} \in \mathbb{R}^{n+1} \mid x_i \geq 0,\ \boldsymbol{x}^T \mathbf{1} = 1 \right\},$$

where $\mathbf{1}$ is a vector of ones of appropriate dimension. Note that $\boldsymbol{x}^T \mathbf{1} = 1 \implies \mathbf{1}^T \boldsymbol{g}(\boldsymbol{x}) = \mathbf{0}$. Hence $\boldsymbol{x}^T \mathbf{1}$ is an invariant hyperplane for the dynamics. Further, the positive orthant $\mathbb{R}^N$ is a trapping region for the dynamics; this follows from the fact that $\dot{x}_i|_{x_i = 0} \geq 0$. The intersection of the invariant hyperplane and the positive orthant of $\mathbb{R}^N$ is the simplex Δ_{N-1}. Hence Δ_{N-1} is a trapping region for the replicator-mutator dynamics (1).

Given the restriction to the simplex Δ_{N-1}, the N-dimensional dynamics can be reduced to an $(N-1)$-dimensional system of equations:

$$\begin{aligned} &\dot{x}_i = h_i(\tilde{\boldsymbol{x}}), \quad i \in \{1, 2, \cdots, N-1\}, \\ &h_i(\tilde{\boldsymbol{x}}) := g_i\left(x_1, x_2, \cdots, x_{N-1}, 1 - \sum_{j=1}^{N-1} x_j\right), \end{aligned} \tag{5}$$

where $\tilde{\boldsymbol{x}} = [x_1, \cdots, x_{N-1}]^T$ and $\boldsymbol{h} : \mathbb{R}^{N-1} \to \mathbb{R}^{N-1}$.

III. DYNAMICS AND BIFURCATION PLOTS

In this section we compute the bifurcations of the dynamics (1) as a function of the bifurcation parameter μ for $N = 2$ and $N = 3$ strategies. We show a transition from

multiple stable dominant equilibria to a unique stable mixed equilibrium for increasing μ, as well as stable limit cycles for $N = 3$.

A. Two Strategies $N = 2$

We summarize the results from [18] for dynamics (1) with two strategies. To simplify notation, define $b_1 := b_{12}$ and $b_2 := b_{21}$. With this notation and following the reduction (5), we have the one-dimensional system

$$\begin{aligned}\dot{x}_1 &= h_1(x_1) = x_1 f_1 q_{11} + x_2 f_2 q_{21} - x_1^2 f_1 - x_1 x_2 f_2 \\ &= x_1\left[b_1 + x_1(1-b_1)\right](1-\mu-x_1) \\ &\quad + (1-x_1)\left[1 + x_1(b_2-1)\right](\mu - x_1).\end{aligned} \tag{6}$$

Figure 1 shows the equilibria of the dynamics (6), and their stability, as a function of the bifurcation parameter μ. The bifurcation plot shows a transition from bistability to a mixed equilibrium via a pitchfork bifurcation in the case $b_1 = b_2$. The pitchfork bifurcation is structurally unstable: for $b_1 \neq b_2$ a saddle-node bifurcation occurs at a critical value μ_c as shown in Figure 1. Three branches of equilibria exist. One of the branches remains stable for all μ and approaches $x_1 = 0.5$ as μ approaches 1. The other two branches exist for $\mu < \mu_c$ and collide in a saddle-node bifurcation at μ_c. Note that $b_1 \neq b_2$ corresponds to a directed payoff graph between the two nodes.

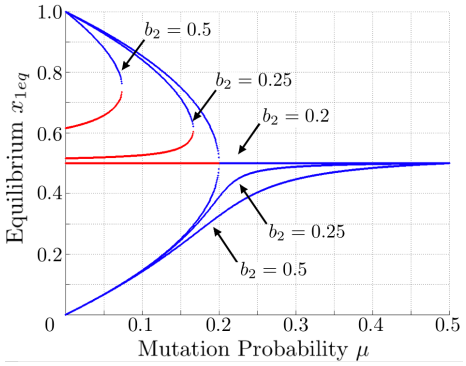

Fig. 1. Three bifurcation plots for $N = 2$ nodes with parameters $b_1 = 0.2$ and $b_2 = 0.2$, 0.25 and 0.5. Blue curves are the stable equilibria and the red curves are the unstable equilibria. Similar to Figure 14 of [18].

B. Three Strategies $N = 3$

Here we consider the three strategy version of the dynamics (1) and constrain the payoff parameters b_{ij} in (3) to be either 0 or equal to a constant value $b > 0$. For $N = 3$, the phase space is planar allowing for the visualization of the codimension-one bifurcations in three dimensions. There are five non-isomorphic graph topologies with three nodes that satisfy the connectivity specified by Condition 1 and have edges of identical weight; these are shown in Figure 2. Figure 2 also shows the bifurcation plots for each of the topologies as a function of the mutation probability μ. Note that for $\mu = 0$ the only stable equilibria for the replicator-mutator system with payoffs (3) are the three pure strategy equilibria. The payoff and mutation matrices for each graph topology are given by (3) and (4) respectively.

1) All-to-all Interconnection: The replicator-mutator dynamics with symmetric all-to-all interconnection and identical weights are studied in detail in [12]. The bifurcation plot Figure 2A has two bifurcation points

$$\begin{aligned}\mu_{C1} &= \frac{2(1-b)}{3(2+b)} \text{ and} \\ \mu_{C2} &= \frac{6+2b}{1-b} - \sqrt{\left(\frac{6+2b}{1-b}\right)^2 - 4}.\end{aligned} \tag{7}$$

At $\mu = \mu_{C1}$ the equilibrium $\boldsymbol{x_{mix}} = \frac{1}{3}\mathbf{1}$ changes stability via an $\mathcal{S}_3$-symmetric transcritical bifurcation [12]. At $\mu = \mu_{C2}$ six equilibria disappear via three symmetric saddle-node bifurcations. Thus for $\mu > \mu_{C2}$ the only remaining equilibrium is the stable $\boldsymbol{x_{mix}}$.

2) Limited Interconnections: The bifurcation plots for graphs in Figures 2B-2D each have a stable branch of equilibria for all μ. They also have two other stable and four unstable equilibria at $\mu = 0$ which disappear in saddle-node bifurcations as μ increases. Small perturbations of the symmetric all-to-all case above yield bifurcations that are qualitatively similar to the limited interconnection cases here and also to the $N = 2$ bifurcations in Figure 1.

3) Directed Cycle Interconnection: The bifurcation plot in Figure 2E corresponds to a directed cycle interconnection among nodes. The equilibrium $\boldsymbol{x_{mix}} = \frac{1}{3}\mathbf{1}$ exists for all values of $\mu \in [0, 1]$. The eigenvalues of the Jacobian of the reduced system (5) evaluated at $(x_1, x_2) = (\frac{1}{3}, \frac{1}{3})$ are

$$\lambda_{1,2} = \frac{1}{3} - \mu - \frac{b}{6} \pm \frac{i}{2\sqrt{3}}(2\mu - b + 2b\mu). \tag{8}$$

At $\mu = \mu_{C1}$ three symmetric saddle-node bifurcations occur and stable limit cycles appear about $\boldsymbol{x_{mix}}$. These are followed by a Hopf bifurcation at $\mu = \mu_{C2}$, where $\boldsymbol{x_{mix}}$ changes stability from an unstable to a stable focus and the limit cycles disappear. The location of the Hopf bifurcation can be computed from the stability of the eigenvalues (8) as

$$\mu_{C2} = \frac{1}{3} - \frac{b}{6}. \tag{9}$$

IV. HOPF BIFURCATION FOR $N = 3$

In this section we formally study the Hopf bifurcation observed in Figure 2E that leads to stable limit cycle behavior. We prove that stable limit cycles of the dynamics exist in a wide region of parameter space for circulant payoff matrices B, for which the directed cycle topology in Figure 2E is a special case. Theorem 1 provides necessary conditions for the existence of limit cycles for (1) with $N = 3$ and circulant B. Lemma 3 shows the existence of the equilibrium $\boldsymbol{x_{mix}} = \frac{1}{N}\mathbf{1}$ for circulant B. Theorem 2 provides sufficient conditions for Hopf bifurcations and stable limit cycles.

A. Necessary conditions for limit cycles

Since the $N = 3$ replicator-mutator dynamics are two-dimensional, Bendixson's Criterion [20] can be used to obtain necessary conditions for the existence of limit cycles. In order to do so we first need to compute the divergence of the vector field, which is given in Lemma 1.

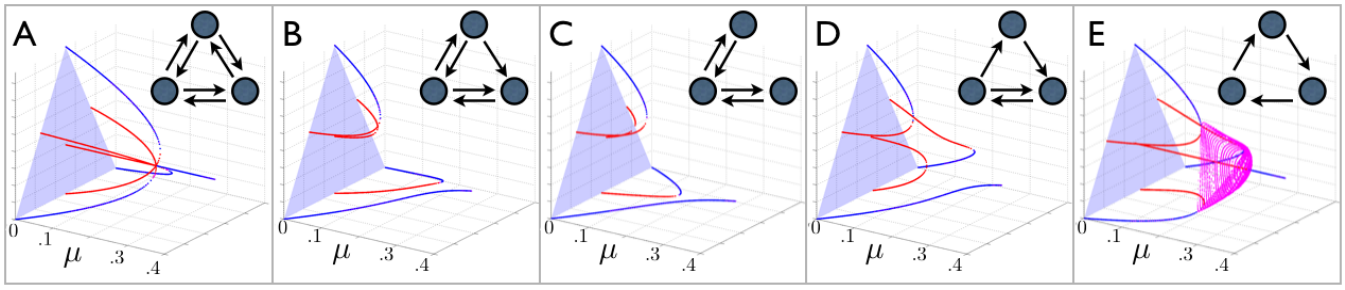

Fig. 2. Bifurcation plots for the $N = 3$ case of dynamics (1) and constant edge weights $b = 0.2$. The x-axis in each plot is the mutation strength μ, blue and red curves are stable and unstable equilibria, respectively, and the magenta curves are stable limit cycles. The three node graphs in each subplot have adjacency matrix B with self-cycles (not shown) at each node.

Lemma 1: The divergence of the vector field $\boldsymbol{g}(\boldsymbol{x})$ restricted to the simplex Δ_{N-1} is given by

$$\nabla \cdot \boldsymbol{g}(\boldsymbol{x})\Big|_{\boldsymbol{x}\in\Delta_{N-1}} = \nabla \cdot \boldsymbol{h}(\tilde{\boldsymbol{x}})$$
$$= \mathbf{1}^T \left[(1-\mu)B + S^T\right]\boldsymbol{x} - \boldsymbol{x}^T\left[NB + B^T\right]\boldsymbol{x},$$

where $S := Q \circ B$, the element-wise product of Q and B.

Proof: The divergence is given by

$$\nabla \cdot \boldsymbol{h}(\tilde{\boldsymbol{x}}) = \sum_{i=1}^{N-1} \frac{\partial h_i}{\partial x_i} = \sum_{i=1}^{N} \frac{\partial g_i}{\partial x_i} - \sum_{i=1}^{N} \frac{\partial g_i}{\partial x_N}. \tag{10}$$

We substitute for $g_i(\boldsymbol{x})$ from (1) in the first term of the difference in (10) and using (3) and (5) we have

$$\sum_{i=1}^{N} \frac{\partial g_i}{\partial x_i} = \sum_i \frac{\partial}{\partial x_i}\left[x_i(f_i q_{ii} - \phi) + \sum_{j\neq i} x_j f_j q_{ji}\right]$$

$$= \sum_i \left[f_i q_{ii} + x_i q_{ii}\frac{\partial f_i}{\partial x_i} - \phi - x_i\frac{\partial \phi}{\partial x_i} + \sum_{j\neq i} x_j q_{ji} b_{ji}\right]$$

$$= (1-\mu)\mathbf{1}^T B\boldsymbol{x} + (1-\mu) - N\phi - \boldsymbol{x}^T(B+B^T)\boldsymbol{x} + \sum_i\sum_{j\neq i} x_j s_{ji}$$

$$= \mathbf{1}^T\left[(1-\mu)B + S^T\right]\boldsymbol{x} - \boldsymbol{x}^T\left[(N+1)B + B^T\right]\boldsymbol{x}. \tag{11}$$

where the last equality follows from the identity $\sum_i\sum_{j\neq i} x_j s_{ji} = \mathbf{1}^T S^T \boldsymbol{x} - (1-\mu)$. Computing the second term in the difference in (10) we have

$$\sum_{i=1}^{N} \frac{\partial g_i}{\partial x_N} = \frac{\partial}{\partial x_N}\left[\sum_{i=1}^{N}\sum_{j=1}^{N} x_j f_j q_{ji} - x_i\phi\right]$$
$$= \frac{\partial}{\partial x_N}\left[(1 - \sum_{i=1}^{N} x_i)\phi\right] = -\phi = -\boldsymbol{x}^T B\boldsymbol{x}. \tag{12}$$

Substituting (11) and (12) in (10) we get the desired result. ■

The remainder of this section specializes to circulant payoff matrices B. A circulant matrix B is fully specified by its first row; the subsequent rows are cyclic permutations of the first row to the right with offset given by the row index. We assume that B is invertible; an $N \times N$ circulant matrix B of the form (3) is always invertible for N prime [21]. Using the divergence calculation from Lemma 1, Lemma 2 gives a necessary condition for the divergence to be negative semi-definite on Δ_{N-1} when B is circulant and invertible. For a circulant matrix B, we define the row sum as $r_B := \sum_{j=1}^{N} b_{ij}$ for any row i.

Lemma 2: Let B be circulant and invertible. Then the divergence $\nabla \cdot \boldsymbol{h}(\tilde{\boldsymbol{x}}) \leq 0$ on the simplex Δ_{N-1} if

$$\mu \geq \frac{(N - r_B)(r_B - 1)}{N\left(r_B^2 - r_{B\circ B}\right)}.$$

Proof: From Lemma 1, the divergence $\nabla \cdot \boldsymbol{h}(\tilde{\boldsymbol{x}})$ is negative semi-definite on the simplex if

$$\max_{x\in\Delta_{N-1}} \mathbf{1}^T\left[(1-\mu)B + S^T\right]\boldsymbol{x} \leq \min_{x\in\Delta_{N-1}} \boldsymbol{x}^T\left[NB + B^T\right]\boldsymbol{x}. \tag{13}$$

The term on the left hand side (LHS) of (13) is the maximum of a convex combination of nonnegative scalars and hence evaluates to

$$\text{LHS} = \max_i \sum_{j=1}^{N}(1-\mu)b_{ji} + s_{ij}$$
$$= (1-\mu)\max_i \sum_{j=1}^{N} b_{ji} + (1-\mu) + \mu \max_i\left[\frac{\sum_{j\neq i} b_{ij}^2}{\sum_{j\neq i} b_{ij}}\right]$$
$$= (1-\mu)(1 + r_B) + \mu\left(\frac{r_{B\circ B} - 1}{r_B - 1}\right). \tag{14}$$

The term on the right hand side (RHS) of (13) is the minimum of a quadratic form that is positive on the simplex. Given that B is circulant and invertible, this quadratic form has an isolated minimum at $\boldsymbol{x_{mix}} = \frac{1}{N}\mathbf{1}$. Thus,

$$\text{RHS} = \min_{x\in\Delta_{N-1}} \boldsymbol{x}^T\left[NB + B^T\right]\boldsymbol{x}$$
$$= \frac{N+1}{N^2}\mathbf{1}^T B\mathbf{1} = \frac{N+1}{N} r_B. \tag{15}$$

Substituting (15) and (14) in (13) gives the desired result. ■

Denote the 3×3 circulant payoff matrix B as B_{C3}:

$$B_{C3} = \begin{bmatrix} 1 & \alpha & \beta \\ \beta & 1 & \alpha \\ \alpha & \beta & 1 \end{bmatrix}, \{\alpha, \beta\} \in [0, 1) \text{ and } \alpha + \beta > 0. \tag{16}$$

Theorem 1 gives a simple necessary condition for the existence of stable limit cycles of the dynamics (1) with $N = 3$ and payoff matrix B_{C3}.

Theorem 1: The dynamics (1) with payoff matrix B_{C3} have no closed orbits in the simplex Δ_2 for

$$\mu > \frac{(2-\alpha-\beta)(\alpha+\beta)}{6(\alpha+\beta+\alpha\beta)} =: \mu_0.$$

Proof: The simplex Δ_2 (a simply connected subset of $\mathbb{R}^2$) is a trapping region for the dynamics (1) (see section II-B). Using Lemma 2 and substituting $r_B = (1+\alpha+\beta)$ and $r_{B\circ B} = (1+\alpha^2+\beta^2)$, the divergence of the vector field on Δ_2 is negative semi-definite for $\mu > \mu_0$. It is easy to check from Lemma 1 that the divergence is not identically equal to zero on Δ_2. Bendixson's Criterion (Theorem 1.8.2 of [20]) then states that no closed orbits can lie in Δ_2 for $\mu > \mu_0$. ■

The all-to-all interconnection topology of Section III-B.1 is a special case of B_{C3} with $\alpha = \beta = b$. Further, the directed cycle case in Section III-B.3 corresponds to $\alpha = b,\ \beta = 0$. In each of the cases, the μ_0 threshold from Theorem 1 evaluates exactly to the critical points μ_{C1} (7) and μ_{C2} (9) respectively.

B. Sufficient conditions for limit cycles

We are now ready to state and prove the main result in Theorem 2 that provides sufficient conditions for the existence of stable limit cycles of the dynamics (1) with payoff matrix B_{C3}. First we show the existence of the equilibrium $\boldsymbol{x_{mix}}$ for circulant B.

Lemma 3: If the payoff matrix B is circulant, then $\boldsymbol{x_{mix}} = \frac{1}{N}\mathbf{1}$ is an equilibrium of the replicator-mutator dynamics (1).

Proof: Suppose B is circulant. Then $\mathbf{1}$ is an eigenvector of B with eigenvalue r_B, i.e., $B\mathbf{1} = r_B\mathbf{1}$. Matrix Q is also circulant by construction from (4). This means that $\sum_{j=1}^{N} q_{ji} = \sum_{j=1}^{N} q_{ij} = 1$. Let $\boldsymbol{x} = \boldsymbol{x_{mix}} = \frac{1}{N}\mathbf{1}$. Then $\boldsymbol{f} = B\boldsymbol{x_{mix}} = \frac{1}{N}B\mathbf{1} = \frac{r_B}{N}\mathbf{1}$. From (1),

$$\dot{x}_i\Big|_{\boldsymbol{x}_{mix}} = \frac{1}{N}\sum_{j=1}^{N} f_j\left(q_{ji} - \frac{1}{N}\right) = \frac{r_B}{N^2}\sum_{j=1}^{N} q_{ji} - \frac{r_B}{N^2} = 0,$$

and $\boldsymbol{x_{mix}} = \frac{1}{N}\mathbf{1}$ is an equilibrium. ■

Theorem 2: Equilibrium $\boldsymbol{x_{mix}}$ of the dynamics (1) with $N = 3$ strategies, payoff matrix B_{C3}, mutation matrix (4) and bifurcation parameter μ, undergoes a supercritical Hopf bifurcation at $\mu = \mu_0$ leading to stable limit cycles for $\mu < \mu_0$ when the following conditions are satisfied:

$$\alpha \neq \beta \qquad \text{(C1a)}$$

$$2\alpha + 2\beta + 5\alpha\beta + \alpha^2 + \beta^2 \neq 2. \qquad \text{(C1b)}$$

Proof: This proof relies on satisfying the conditions of the two-dimensional Hopf bifurcation theorem (Theorem 3.4.2 from [20]). The stability term $\ell_1(\alpha,\beta)$ is the first Lyapunov coefficient [22] of the dynamics.

For $N = 3$, the dynamics (1) evolve on $\Delta_2 \subset \mathbb{R}^2$ and are denoted $\dot{x}_i = h_i(x_1, x_2)$, $i \in \{1, 2\}$ as in (5). From Lemma 3 we have that $(x_1, x_2) = (\frac{1}{3}, \frac{1}{3}) =: \boldsymbol{x_0}$ is an equilibrium of the dynamics since B_{C3} is circulant. The Jacobian of the vector field $\boldsymbol{h}$ evaluated at $\boldsymbol{x_0}$ has eigenvalues

$$\lambda(\alpha,\beta,\mu) = \left[\frac{1}{3} - \mu - \frac{1}{6}(\alpha+\beta) - \frac{\alpha\beta}{\alpha+\beta}\mu\right] \pm i\left[\frac{1}{2\sqrt{3}}\frac{\alpha-\beta}{\alpha+\beta}\{(\alpha+\beta-2\mu(1+\alpha+\beta)\}\right].$$

Let $\tilde{\mu} = \frac{\alpha+\beta}{2(1+\alpha+\beta)}$. The eigenvalues $\lambda(\alpha,\beta,\mu)$ satisfy the following:

$$\text{Re}\left[\lambda(\alpha,\beta,\mu)\right] = 0 \iff \mu = \mu_0$$

$$\text{Im}\left[\lambda(\alpha,\beta,\mu)\right] \neq 0 \iff \mu \neq \tilde{\mu} \text{ and } \alpha \neq \beta.$$

The conditions $\alpha \neq \beta$ and $\tilde{\mu} \neq \mu_0$ are precisely (C1a) and (C1b) respectively, which together imply that $\lambda(\alpha,\beta,\mu_0)$ are purely imaginary. This satisfies property (H1) of the Hopf bifurcation theorem.

Property (H2) of the theorem requires that the complex eigenvalues cross the imaginary axis with nonzero *velocity* v_0. This is also satisfied since

$$v_0 := \frac{d}{d\mu}\left(\text{Re}\ \lambda(\alpha,\beta,\mu)\right)\Big|_{\mu=\mu_0} = \frac{-(\alpha+\beta+\alpha\beta)}{\alpha+\beta} \neq 0.$$

Since (C1a) and (C1b) imply that (H1) and (H2) of the Hopf bifurcation theorem are satisfied, we conclude that the dynamics undergo a Hopf bifurcation at $\mu = \mu_0$. The limit cycles arising out the Hopf bifurcation are stable if the first Lyapunov coefficient $\ell_1(\alpha,\beta)$ evaluated at $\boldsymbol{x_0}$ and μ_0 is negative. We compute $\ell_1(\alpha,\beta) = \frac{3(\alpha+\beta-2)}{\omega_0}$, where,

$$\omega_0 = |\tilde{\omega}|,\ \ \tilde{\omega} = \frac{(\alpha-\beta)(\alpha^2+\beta^2+2\alpha+2\beta+5\alpha\beta-2)}{6\sqrt{3}(\alpha+\beta+\alpha\beta)}.$$

This implies (C1a) and (C1b) $\iff \ell_1(\alpha,\beta) < 0$.

From Theorem 1 we know that the dynamics have no limit cycles for $\mu > \mu_0$. Thus we have proved the existence of stable limit cycles for $\mu < \mu_0$. ■

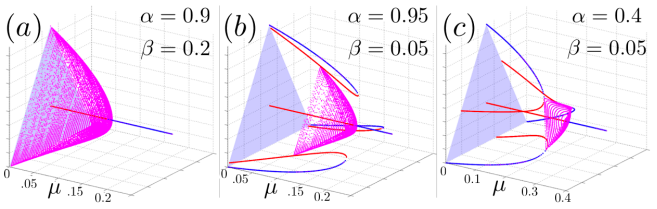

Fig. 3. Bifurcation plots for the dynamics (1), payoff matrix B_{C3} and parameters α and β as shown. The existence of Hopf bifurcations and stable limit cycles for the set of parameter choices follows from Theorem 1. Note the coexistence of stable equilibria with stable limit cycles in Figure 3b.

Figure 2E shows limit cycles for a specific case of B_{C3} with $\alpha = b$ and $\beta = 0$. Figure 3 shows three more limit cycle bifurcation plots for nonzero α and β. Interestingly, for selected parameter values in Figure 3b stable limit cycles coexist with multiple stable equilibria. This coexistence of stable equilibria and stable limit cycles implies that different initial conditions can yield qualitatively distinct limiting behavior even with fixed parameters for the dynamics (i.e. without bifurcations).

V. BEYOND CIRCULANT PAYOFFS

It is important to note that studying the fully general model (1), even with $N = 3$ strategies, is highly complex. This complexity motivated our restriction to payoff matrices of the form B_{C3} which can be fully characterized in terms of just two parameters and allowed for a careful bifurcation analysis of the dynamics as presented in the previous section. Nonetheless, the analysis in Section IV might lead one to conclude that the circulant structure of payoff matrix B_{C3} is a *necessary* condition for Hopf bifurcations of the dynamics. In this section we illustrate that this is not the case. We show examples of limit cycles for selected non-circulant payoff matrices. Consider 3×3 payoff matrices B satisfying (3) and Condition 1 that have have directed links of two kinds: strong links with weights b and weak links with weights ϵb where $b \in (0, 1)$ and $0 < \epsilon \ll 1$. There are 73 corresponding non-isomorphic graph topologies. Figure 4 shows stable limit cycles for four topologies in this set corresponding to non-circulant payoff matrices.

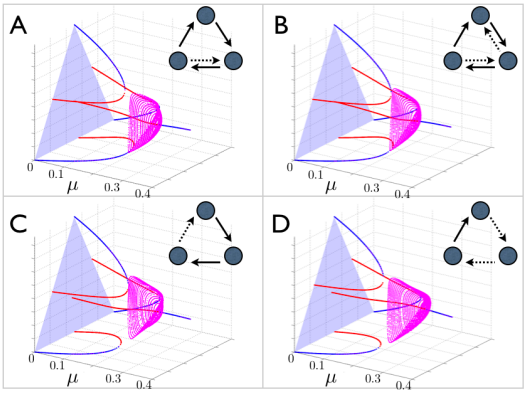

Fig. 4. Limit cycles for non-circulant payoff matrices B. The solid arrows in the graphs are strong links with weight b and the dashed arrows are weak links with weight ϵb. Parameters for all plots are $b = 0.2$ and $\epsilon = 0.1$.

VI. FINAL REMARKS

Much of the analysis of the replicator-mutator dynamics has been focused on stable equilibrium limiting behavior. The analysis has also primarily considered payoff and mutation matrices that are symmetric, which corresponds to undirected graph topologies between strategy nodes. Recent work [10] on a graph theoretic model of the language dynamics has shown that the graph connectivity plays a critical role in determining the location of bifurcation points in the dynamics, but the restriction to undirected graphs confines the range of limiting behavior to stable equilibria. The paper by Mitchener and Nowak [19] has served as important motivation for this work. The authors show that considering asymmetric payoff and mutation matrices (corresponding to directed graphs) can yield limit cycle behavior and even chaos for replicator-mutator dynamics. Here we prove conditions such that stable limit cycles arise as a consequence of Hopf bifurcations for $N = 3$ strategies and circulant payoff matrices. From a graph perspective, we show how breaking symmetry by considering directed graphs allows for oscillatory limiting behavior for the replicator-mutator dynamics.

We emphasize that the limit cycles are not restricted to circulant payoffs or to $N = 3$, but can exist for non-circulant payoffs as shown in Section V, and for larger networks with random payoffs as shown in Figure 5. A Hopf bifurcation analysis of these more general cases is an intended future direction.

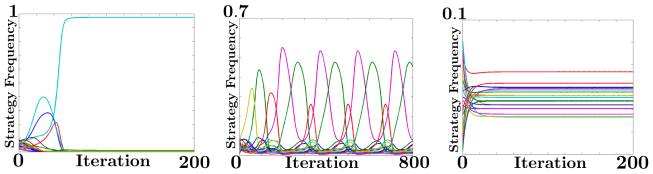

(a) $\mu = 0.01$ (b) $\mu = 0.15$ (c) $\mu = 0.4$

Fig. 5. Simulation of the dynamics (1) for $N = 20$ nodes and $b_{ij} \in [0, 1)$ chosen randomly. Notice the transition from a highly coherent state for small μ, to oscillating dominance for intermediate μ and eventually to a mixed state for large μ.

REFERENCES

[1] M.A. Nowak, N.L. Komarova, and P. Niyogi. Evolution of universal grammar. *Science*, 291(5501):114, 2001.

[2] R. Olfati-Saber. Evolutionary dynamics of behavior in social networks. In *46th IEEE Conf. on Decision & Control*, pages 4051–4056, 2007.

[3] I. Hussein. An individual-based evolutionary dynamics model for networked social behaviors. In *Proceedings of the American Control Conference*, pages 5789–5796, 2009.

[4] H. Tembine, E. Altman, R. El-Azouzi, and Y. Hayel. Evolutionary games in wireless networks. *IEEE Transactions on Systems, Man, and Cybernetics, Part B*, 40(3):634–646, 2010.

[5] T.L. Vincent and T.L.S. Vincent. Evolution and control system design: the evolutionary game. *Control Systems Magazine, IEEE*, 20(5):20–35, 2002.

[6] M.A. Nowak and K. Sigmund. Evolutionary dynamics of biological games. *Science's STKE*, 303(5659):793, 2004.

[7] J. Hofbauer and K. Sigmund. Evolutionary game dynamics. *Bulletin of the American Mathematical Society*, 40(4):479, 2003.

[8] P.D. Taylor and L.B. Jonker. Evolutionary stable strategies and game dynamics. *Mathematical Biosciences*, 40(1-2):145–156, 1978.

[9] K.M. Page and M.A. Nowak. Unifying evolutionary dynamics. *Journal of Theoretical Biology*, 219(1):93–98, 2002.

[10] Y. Lee, T. Collier, C. Taylor, and R. Olfati-Saber. Simplicity from complexity: emergence of cohesion in the evolutionary dynamics of grammar networks. *Evolutionary Ecology*, 11(3):433–445, 2009.

[11] N.L. Komarova, P. Niyogi, and M.A. Nowak. The evolutionary dynamics of grammar acquisition. *Journal of Theoretical Biology*, 209(1):43–59, 2001.

[12] W. Garrett Mitchener. Bifurcation analysis of the fully symmetric language dynamical equation. *Journal of Mathematical Biology*, 46(3):265–285, 2003.

[13] W. Mitchener. *A Mathematical Model of Human Languages: The interaction of game dynamics & learning processes*. Princeton University, 2003.

[14] J. Hofbauer and K. Sigmund. *Evolutionary Games and Replicator Dynamics*. Cambridge University Press, 1998.

[15] A.J. Bladon, T. Galla, and A.J. McKane. Evolutionary dynamics, intrinsic noise, and cycles of cooperation. *Physical Review E*, 81(6):66122, 2010.

[16] A. Traulsen, J.C. Claussen, and C. Hauert. Coevolutionary dynamics in large, but finite populations. *Physical Review E*, 74(1):11901, 2006.

[17] Y. Wang and I Hussein. Evolutionary bandwidth allocation and routing in large-scale wireless sensor networks. In *American Control Conference, 2010*, pages 1850–1855, 2010.

[18] N.L. Komarova and S.A. Levin. Eavesdropping and language dynamics. *Journal of Theoretical Biology*, 264(1):104–118, 2010.

[19] W.G. Mitchener and M.A. Nowak. Chaos and language. *Proceedings of the Royal Society B: Biological Sciences*, 271(1540):701, 2004.

[20] J. Guckenheimer and P. Holmes. *Nonlinear Oscillations, Dynamical Systems, and Bifurcations of Vector Fields*. Springer, 2002.

[21] R. Horn and C. Johnson. *Matrix Analysis*. Cambridge U. Press, 1990.

[22] Y. Kuznetsov. *Elements of Applied Bifurcation Theory*. Springer, 1998.